[CANCER RESEARCH 64, 2717–2724, April 15, 2004]

Activation of the Tumor Suppressor Merlin Modulates Its Interaction with Lipid Rafts

John T. Stickney, W. Clark Bacon, Meghan Rojas, Nancy Ratner, and Wallace Ip

Department of Cell Biology, Neurobiology, and Anatomy, Vontz Center for Molecular Studies, University of Cincinnati College of Medicine, Cincinnati, Ohio

ABSTRACT

Neurofibromatosis type 2 (NF2) is a genetic disorder characterized by bilateral schwannomas of the eighth cranial nerve. The *NF2* tumor suppressor protein, merlin, is related to the ERM (ezrin, radixin, and moesin) family of membrane/F-actin linkers. Merlin resists solubilization by the detergent Triton X-100 (TX-100), a property commonly attributed to association with the cytoskeleton. Accordingly, NF2 patient mutations that encode merlins with enhanced TX-100 solubility have been explained previously in terms of loss of cytoskeletal attachment. However, here we present data to suggest that the detergent resistance of merlin is a result of its constitutive residence in lipid rafts. Furthermore, when cells are grown to high density, merlin shifts to a more buoyant lipid raft fraction in a density gradient. This shift is mimicked in subconfluent cells treated with cytochalasin D, suggesting that the shift results from merlin dissociation from the actin cytoskeleton, but not from lipid rafts. Intramolecular NH_2- and COOH-terminal binding, which occurs when merlin transitions to the growth-suppressive form, also brings about a similar change in buoyant density. Our results suggest that constitutive residence of merlin in lipid rafts is crucial for its function and that as merlin becomes growth suppressive *in vivo*, one significant molecular event may be the loss of interaction with the actin cytoskeleton. To our knowledge, merlin is the first tumor suppressor known to reside within lipid rafts, and the significance of this finding is underscored by known loss-of-function NF2 patient mutations that encode merlins with enhanced TX-100 solubility.

INTRODUCTION

Merlin (schwannomin) is the M_r ~70,000 tumor suppressor protein product of the neurofibromatosis type 2 (*NF2*) gene (1, 2). *NF2* is inherited as an autosomal dominant trait with an incidence of approximately 1 in 40,000. Individuals suffering from NF2 have characteristic benign schwannomas arising on the eighth cranial nerve, schwannomas of other cranial nerves and peripheral nerves, as well as increased incidence of meningiomas and spinal ependymomas. *Nf2* knockout mice die *in utero* (3), and mice heterozygous for an *Nf2* mutation demonstrate an increased propensity for osteosarcoma, fibrosarcoma, and hepatocellular carcinoma formation (4). Additionally, mice in which both *Nf2* alleles are conditionally inactivated in Schwann cells using the CRE/loxP system develop Schwann cell hyperplasia and schwannomas (5). These data, coupled with the report of widespread merlin expression *in vivo* (6), implicate merlin as a crucial growth regulator for numerous cell and tissue types. Precisely how merlin suppresses tumor growth, however, has yet to be fully elucidated.

Merlin is a member of the band 4.1/ERM (ezrin, radixin, and moesin) family of plasma membrane/actin cytoskeleton linkers. The ERM proteins and merlin possess NH_2-terminal four-point-one, ezrin, radixin, moesin (FERM) domains that mediate interaction with integral membrane proteins including the hyaluronate receptor, CD44 (7). The COOH-termini of the ERM proteins are characterized by a conserved actin-binding motif that is absent in merlin. Merlin and ERM proteins can self-associate to form homodimers or heterodimerize with one another (8–10). Intra-/intermolecular association is believed to regulate their activity (7). Despite their sequence similarity and ability to associate, overexpression of merlin results in suppression of cell growth, whereas overexpression of ezrin is correlated with cell proliferation (7).

Like ERM proteins, merlin exists in two conformations (open and closed), but in contrast to the ERM proteins, merlin is believed to be active (growth suppressive) in its closed conformation (10). Conversion of merlin to the open, inactive form is mediated by phosphorylation (11). Strong evidence exists that merlin plays a role in cell density-dependent growth arrest, with conversion from the inactive to active conformation occurring with increasing cell density (12).

In many cell types, merlin is enriched within actin-rich membrane ruffles (13–15). Cultured schwannoma cells, which lack merlin, have an aberrant ruffling phenotype (14) that can be corrected by the addition of exogenous merlin (16, 17), suggesting a role for merlin in cellular actin dynamics. Merlin lacks the COOH-terminal actin-binding motif present in the ERM proteins, so it clearly lacks the capacity to bind actin in the same way that ERM proteins do. It is far less clear, however, if merlin binds actin directly, and what the physiological significance of the reported (3, 14) interaction of merlin with actin via its NH_2-terminal FERM domain might be (18). Current evidence appears to favor the interpretation that indirect binding may be possible but that direct merlin/actin binding *in vivo* is unlikely (19).

Merlin is insoluble in the nonionic detergent Triton X-100 (TX-100; Ref. 20). Moreover, *NF2* patient mutations have been described that render merlin more soluble in TX-100 (15, 21). Historically, insolubility in nonionic detergents has been viewed as an indicator of association with the cytoskeleton. Not surprisingly, therefore, the molecular defect of such *NF2* mutations has been assumed to be weakened association with the cytoskeleton. However, studies in the last decade have shown that certain microdomains of the plasma membrane and, to some extent, internal membranes are also resistant to solubilization in nonionic detergents because of their uniquely tight packing of glycosphingolipids and cholesterol moieties (22). Such microdomains are aptly called detergent-resistant membranes (DRMs), and they fall into two main subclasses, lipid rafts and caveolae. Proteins that associate with DRMs would also be expected to be detergent insoluble. Prominent among such proteins are key players in known signal transduction pathways (*e.g.*, integrins and the Src family kinases) and membrane trafficking (22). Prevailing opinion is that concentration of signaling proteins in a physical "platform" increases the specificity and efficiency of their interactions and thus enhances the signaling event (22).

Because there is strong evidence that merlin is involved in a number of signaling pathways (18, 23), and because known merlin-binding partners have been localized to DRMs (24), we sought to determine whether merlin was localized to DRMs, and whether this could account for the previously reported detergent resistance of

Received 12/4/03; revised 1/27/04; accepted 2/11/04.

Grant support: NIH Grant R01-CA75824 (W. Ip and N. Ratner) and Department of Defense CDMRP Grant NF020037 (W. Ip). J. T. Stickney was supported by National Institute of Environmental Health Sciences Training Grant ES07250 awarded to P. J. Stambrook and is currently the recipient of a Young Investigator Award from the National Neurofibromatosis Foundation. W. C. Bacon was supported by National Cancer Institute Training Grant T32 CA059268 awarded to S. A. Khan.

The costs of publication of this article were defrayed in part by the payment of page charges. This article must therefore be hereby marked *advertisement* in accordance with 18 U.S.C. Section 1734 solely to indicate this fact.

Requests for reprints: Wallace Ip, Department of Cell Biology, Neurobiology, and Anatomy, University of Cincinnati College of Medicine, 3125 Eden Avenue, Cincinnati, OH 45267. Phone: (513) 558-3614; Fax: (513) 558-4454; E-mail: wallace.ip@uc.edu.

merlin. We found that the bulk of cellular merlin is localized within lipid rafts, whereas virtually no ezrin was DRM associated. Our data also indicate that raft residence, not actin association, is primarily responsible for the detergent resistance of merlin. Additionally, although merlin is constitutively localized to lipid rafts, the buoyant density of merlin-containing lipid rafts changes with cell density and with the conversion of merlin from the open, inactive conformation to the closed, active conformation. This change likely reflects a dissociation of merlin-containing lipid rafts from cytoskeletal proteins and suggests that, as merlin becomes growth suppressive *in vivo*, a significant molecular event may be the loss of interaction with the actin cytoskeleton (11). Our observations indicate, however, that this important transition occurs within the signaling-rich environment of lipid rafts.

MATERIALS AND METHODS

Reagents and Supplies. Unless noted, all reagents were purchased from Sigma. Polyclonal anti-Fyn (SC-16) was purchased from Santa Cruz Biotechnology, polyclonal anti-caveolin was purchased from BD Biosciences, monoclonal anti-green fluorescent protein was purchased from Roche, monoclonal anti-ezrin was purchased from Sigma, monoclonal anti-T7 was purchased from Novagen, and monoclonal anti-hemagglutinin was purchased from Covance. N3 enhanced green fluorescent protein (eGFP) vector was purchased from ClonTech, and pcDNA3 vector was purchased from Invitrogen. Fluorescence-conjugated secondary antibodies and phalloidin were purchased from Molecular Probes. Horseradish peroxidase-conjugated secondary antibodies and the SuperSignal West Pico Chemiluminescent immunoblot detection kit were purchased from Pierce. *N*-Octyl-β-D-glucopyranoside (n-OG) was purchased from Fisher.

Cell Culture. U251 cells (a gift from Dr. Steven Berberich, Wayne State University) and NIH3T3 cells were maintained in DMEM (Life Technologies, Inc.) supplemented with 10% FCS (United States Bio-Technologies Inc.) and 100 units/ml penicillin/streptomycin (Life Technologies, Inc.). Transient transfection was carried out using LipofectAMINE 2000 (Life Technologies, Inc.) according to the manufacturer's directions. To create merlin-eGFP-expressing clonal cell lines, 10^5 U251 cells were plated on 6-well plates and then transfected using LipofectAMINE 2000. On the following day, cells were trypsinized and replated onto 100-mm dishes in medium containing 250 μg/ml G418, and fluorescent colonies were isolated. Expression of fusion proteins of the expected length was confirmed by Western blot analysis.

DNA Cloning. Full-length merlin isoform I (growth-suppressive form) was amplified from a modified pBluescript vector (pMKS) using PCR and cloned into an eGFP vector (N3 vector; ClonTech) using *Sal*I and *Bam*HI. When expressed in cells, the construct encoded a fusion protein of merlin fused to the NH_2 terminus of eGFP (merlin-eGFP). T7 epitope-tagged NH_2-terminal merlin and hemagglutinin-tagged COOH-terminal merlin constructs were created by including codons for these epitopes in the 5′ region of sense strand primers used for amplification. *Bam*HI and *Eco*RI sites were also included in 5′ ends of sense and antisense primers, respectively, for directional cloning of PCR products into pcDNA3.

Immunofluorescence. Cells (2×10^4) were plated onto glass coverslips and allowed to adhere overnight. The following morning, cells were removed from the incubator, and the subsequent steps were performed at room temperature. Cells were washed twice in Tris-buffered saline (TBS) and then fixed using 4% paraformaldehyde in PBS for 10 min, followed by permeabilization using ice-cold 1% TX-100 in TBS for 3 min. The order of addition was reversed for cells that were detergent extracted before fixation. Coverslips were blocked using 5% nonfat milk in TBS for 30 min and then incubated in primary antibody in TBS (1:250 for caveolin, 1:100 for Fyn) for 1 h. After three washes with TBS, fluorescence-conjugated secondary antibody (1:1000 in TBS) was added for 1 h, followed by three washes in TBS, one wash in water, and mounting onto slides. For labeling of F-actin, fluorescence-labeled Alexa 633 phalloidin (Molecular Probes) was used per manufacturer's directions.

Subcellular Fractionation and Detergent Extraction of Cells. S100/P100 fractionation was performed as described previously (25) using 10^6 NIH3T3 cells on 60-mm dishes transfected with epitope-tagged merlin expression constructs. After centrifugation, the S100 supernatant (cytosol) was removed, and proteins were precipitated by the addition of 4 volumes of cold acetone. To extract TX-100-soluble membrane proteins, the P100 pellet was resuspended in 200 μl of ice-cold 1% TX-100 in TBS and placed on ice for 15 min. The TX-100-resistant material was pelleted at 14,000 rpm in a microcentrifuge at 4°C for 15 min. To solubilize DRM proteins, the TX-100-resistant pellet was resuspended in 200 μl of ice-cold 100 mM n-OG in TBS and placed on ice for 15 min followed by a 15-min centrifugation in a microcentrifuge as described above. Pellets were resuspended in 200 μl of 1% TX-100/TBS, and then 200 μl of 2× SDS-PAGE sample buffer were added to each fraction, and tubes were boiled for 5 min. Equal volumes of each fraction were loaded for SDS-PAGE analysis. For TX-100 solubility analysis of U251 cells, 2×10^6 clonal cells expressing merlin-eGFP were plated per well of a 6-well plate and allowed to adhere overnight. Cells were collected as described above and lysed in 200 μl of ice-cold 1% TX-100 followed by 15 min of centrifugation in a microcentrifuge. Pellets were resuspended in 200 μl of 1% TX-100/TBS, and all tubes were prepared for SDS-PAGE as described above.

Optiprep Density Centrifugation. Density centrifugation was adapted from Oliferenko *et al.* (24). Clonal U251 cells (2×10^6) expressing merlin-eGFP were plated onto 100-mm plates and allowed to adhere overnight. For NIH3T3 cells, 10^6 cells were plated on 35- or 100-mm plates and then transfected with merlin-eGFP for cell density experiments or plated on 60-mm plates for epitope-tagged NH_2- and COOH-terminal expression experiments. Twenty-four h after transfection, cells were washed two times with TBS, lysed in 267 μl of ice-cold Optibuffer [50 mM Tris (pH 7.5), 150 mM NaCl, 10% sucrose, 1 mM DTT, 1% TX-100, 1 mM phenylmethylsulfonyl fluoride, and protease inhibitor mixture), and then transferred to microcentrifuge tubes and put on ice for 30 min. We added 533 μl of 60% Optiprep to the samples (to a final concentration of 40%), and lysates were transferred to ultracentrifuge tubes. A gradient was created by the sequential layering of 800 μl of 35%, 30%, 25%, 20%, and 0% Optiprep diluted in Optibuffer on top of the samples. Samples were spun at 30,000 rpm ($>107{,}000 \times g$) for 18 h at 4°C in an SW50.1 rotor. After centrifugation, 800-μl fractions were removed in reverse order of addition. Eighty μl of each fraction were mixed with 20 μl of 5× SDS-PAGE sample buffer and boiled for 5 min. Forty μl were loaded per well of a 4–12% NuPAGE precast SDS-PAGE gel (Invitrogen).

Immunoblot Analysis. After SDS-PAGE, proteins were transferred to nitrocellulose and blocked overnight at 4°C using 5% nonfat milk diluted in TBS containing 0.5% Tween 20 (TBST). Subsequent steps were carried out at room temperature. After three 5-min washes in TBST, primary antibody diluted in blocking solution was added, and blots were rocked for 1 h. Antibodies were diluted as follows: anti-green fluorescent protein, 1:1,000; anti-ezrin, 1:4,000; anti-caveolin, 1:5,000; anti-hemagglutinin, 1:1,000; and anti-T7, 1:10,000. Blots were then washed six times, 5 min each, and then rocked for 1 h in horseradish peroxidase-conjugated secondary antibody (diluted 1:10,000 in blocking solution). After six 5-min washes, horseradish peroxidase was detected by a 10-min incubation with enhanced chemiluminescence reagent followed by exposure to X-ray film.

Cholesterol Depletion and Actin Disruption. For cholesterol depletion, cells were washed two times with HBSS and then incubated with DMEM with or without 10 mM methyl-β-cyclodextrin (CD) and returned to the incubator for 30 min. Disruption of cellular F-actin was carried out by the addition of cytochalasin D for 90 min to a final concentration of 10 μM.

RESULTS

Previous workers (9, 13, 14, 26, 27) noted a high degree of localization of merlin in some, but not all, F-actin-containing subcellular domains. We further examined this issue by a confocal microscope immunocytochemical analysis of U251 cells expressing eGFP-tagged merlin. As reported previously, merlin and actin frequently, but not always, colocalized at cortical regions of the cell. Additionally, we detected a previously overlooked mode of merlin localization: a finely dispersed and punctate fluorescent pattern extending over large expanses of the cell membrane (Fig. 1*A*, *top row*). This was not an artifact associated with the fusion of merlin to eGFP because cells transfected with a vector encoding eGFP alone showed uniform and

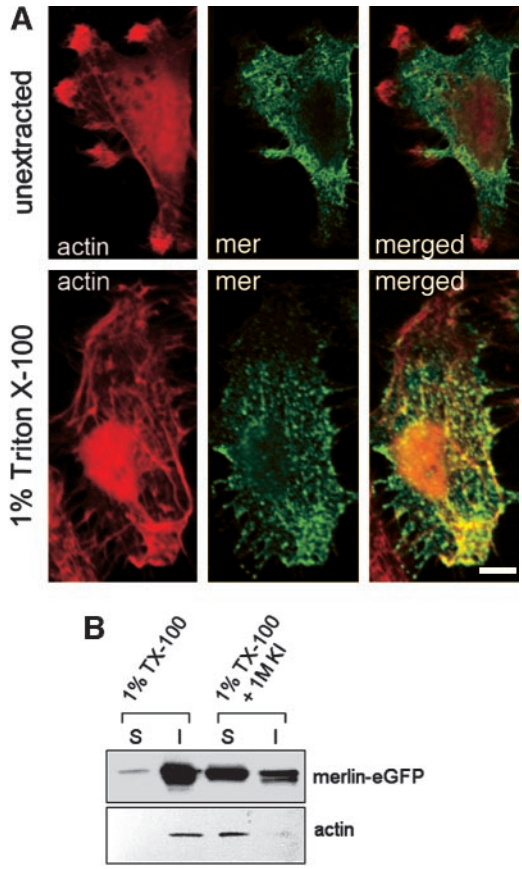

Fig. 1. Merlin detergent resistance is partially dependent on F-actin. *A*, cells were fixed either before (*top row*) or after (*bottom row*) extraction with cold 1% Triton X-100 and imaged by confocal microscopy. F-actin, labeled with Alexa 633-phalloidin, is shown in *red*; merlin-enhanced green fluorescent protein is shown in *green*. Optical sections were taken at the level of the ventral plasma membrane, adjacent to the coverslip. The merged image is shown at the *right*, where areas of actin-merlin colocalization appear *yellow*. The *scale bar* represents 10 μm. *B*, P100 fractions from 10^6 NIH3T3 cells expressing merlin-enhanced green fluorescent protein were extracted with 1% Triton X-100 in Tris-buffered saline with or without 1 M potassium iodide to depolymerize F-actin. Whereas potassium iodide treatment does appear to increase the solubility of merlin, note that a significant population of merlin remains detergent resistant after actin depolymerization (*+1M KI*).

diffuse fluorescence throughout the cytoplasm, with no specific localization to subcellular structures (data not shown).

It is important to note that although this pattern of merlin localization has not been described previously, it is fully consistent with published images of merlin localization. The images of U251 cells immunolabeled for endogenous merlin in Sainio *et al.* (27) and Gronholm *et al.* (9), although lower in magnification, strongly suggest a punctate merlin pattern in both subconfluent and confluent cultures. Similarly, the images presented by Schmucker *et al.* (26) of human foreskin fibroblasts immunostained for endogenous merlin using a commercial anti-merlin antibody, sc332 (Santa Cruz Biotechnology), show a punctate pattern at the plasma membrane.

To determine whether the punctate merlin-containing structures were associated with F-actin, merlin-eGFP-expressing cells were extracted with cold 1% TX-100 before fixation and labeling for F-actin. Confocal images taken at or near the plasma membrane (Fig. 1*A*, *bottom row*) showed that the punctate pattern of merlin localization was even more pronounced after TX-100 extraction. Moreover, many of the puncta appeared to align with actin-containing stress fibers, a feature not readily observable in unextracted cells (Fig. 1*A*). This suggested that removal of the TX-100-soluble portion of the plasma membrane resulted in an aggregation of merlin-containing membranes, many of which appeared to colocalize with F-actin.

To further investigate the interrelationship between merlin and the microfilament network, we transfected NIH3T3 cells with merlin-eGFP and prepared P100 fractions containing cellular membranes and cytoskeletal elements. This fraction was resuspended in TBS containing the nonionic detergent 1% TX-100 and separated into soluble (*S*) and insoluble (*I*) components (Fig. 1*B*). In agreement with previous results (15, 23), merlin was virtually insoluble in 1% TX-100. We further reasoned that if the detergent resistance of merlin was due to direct association of merlin with F-actin, as has been assumed by previous workers (23, 28), then disruption of the F-actin network should result in the solubilization of merlin in TX-100. To test this hypothesis, we included 1 M potassium iodide (KI) in the Triton extraction buffer to depolymerize F-actin (29). Although this treatment effectively solubilized all of the F-actin, a significant amount of merlin remained in the insoluble fraction (Fig. 1*B*). This suggested the presence of two TX-100-insoluble pools of cellular merlin: an F-actin-associated pool; and a second pool that is detergent resistant for reasons other than association with F-actin.

One possibility for the observed actin-independent detergent resistance of merlin was localization of merlin to DRMs. DRMs are plasma membrane microdomains involved in numerous signal transduction processes, and, similar to cytoskeletal elements, they resist solubilization by nonionic detergents such as TX-100 (30, 31). We examined the putative localization of merlin to DRMs by means of a solubility assay. NIH3T3 cells expressing merlin-eGFP were first separated into cytosolic (S100) and membrane-bound (P100) fractions. The P100 pellet was then separated into TX-100-soluble, n-OG (a detergent known to solubilize some DRMs; Ref. 32)-soluble, and detergent-resistant fractions. The various fractions were then subjected to immunoblot analysis (Fig. 2*A*). In agreement with published results on non-epitope-tagged merlin (15), virtually no merlin-eGFP was found in the cytosolic fraction, and only a minute amount was found to be soluble in TX-100 (Fig. 2*A*). In contrast, under these experimental conditions, ezrin was nearly completely cytosolic (Fig. 2*A*), as was eGFP alone (data not shown). This is consistent with previous data suggesting that the bulk of cellular ezrin is cytoplasmic (33) and that the ezrin (and possibly other ERM proteins) localized to DRMs likely represents only a small fraction of the total cellular ezrin (34). On the other hand, the essentially complete resistance of merlin to cold TX-100 and partial solubility in n-OG argued that a significant proportion of the cellular merlin was resident in DRMs (Fig. 2*A*). These solubility properties are nearly identical to those of several proteins recently identified to be within DRM-H, a subset of DRMs in neutrophils that were partially soluble in n-OG and had slightly higher density due to attachment to the membrane skeleton (35).

Density gradient fractionation of U251 cells expressing merlin-eGFP was performed to confirm the localization of merlin to DRMs. DRMs and their associated proteins float to the top of density gradients and can thus be distinguished from the bulk of cellular material. When U251 cells expressing merlin-eGFP were lysed with cold 1% TX-100 and then separated on an Optiprep density gradient, merlin-eGFP was found primarily in the DRM-containing 20% and 25% fractions (Fig. 2*B*), consistent with localization to lipid rafts. Ezrin (as well as free green fluorescent protein; data not shown) was found in the 35% and 40% fractions, as expected for a cytoplasmic, TX-100-soluble protein (Fig. 2*A*). It is important to note that the density gradients were performed using total cell lysates that were not further fractionated. Thus, the preponderance of merlin in the 20% and 25% fractions indicates that essentially all cellular merlin is localized to DRMs.

DRM organization is dependent on the presence of cholesterol. Treatment with the cholesterol-sequestering reagent CD destabilizes DRMs and can render DRM-associated proteins more soluble in

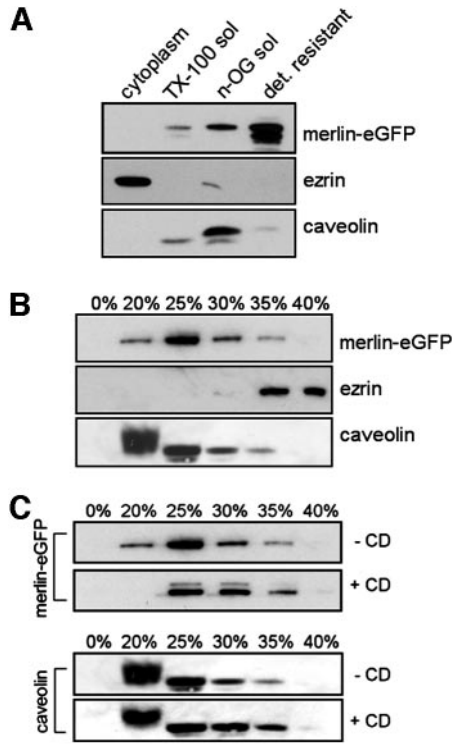

Fig. 2. Merlin resides in detergent-resistant membranes (DRMs). *A*, 10^6 NIH3T3 cells on 60-mm dishes were transfected with merlin-enhanced green fluorescent protein (eGFP) or eGFP (data not shown) and then separated into S100 (cytoplasm) and P100 fractions. The Triton X-100-soluble (*TX-100 sol*) proteins from the P100 fraction were extracted, and then the remainder of the material was resuspended in *N*-octyl-β-D-glucopyranoside to solubilize DRM components (*n-OG sol*). The material that remained after *N*-octyl-β-D-glucopyranoside treatment is labeled detergent resistant (*det. resistant*). Note the distinct difference between the solubility of ezrin and merlin. *B*, 2×10^6 clonal U251 cells expressing merlin-eGFP were plated on 100-mm dishes and allowed to adhere overnight before separation in an Optiprep gradient. Merlin is predominantly found in the 20% and 25% fractions, a hallmark of DRM-associated proteins. Ezrin, as a soluble cytosplasmic protein (see *A*), remains in the 35% and 40% fractions. Caveolin is shown as a positive control for flotation of DRM-associated proteins. *C*, 2×10^6 clonal U251 cells expressing merlin-eGFP were plated on 100-mm dishes and allowed to adhere overnight. Cells were then treated with 10 mM methyl-β-cyclodextrin (CD) for 30 min to disrupt lipid raft structure (*+CD*), or treated with vehicle alone (*−CD*), and fractionated in an Optiprep gradient. Note the disappearance of merlin from the 20% lipid raft fraction of CD-treated cells and a similar (albeit slighter) shift of caveolin to heavier fractions.

TX-100 (36). CD treatment of U251 cells resulted in a 2-fold increase in the amount of Triton-soluble merlin-eGFP (data not shown). This modest increase supports the idea that intact lipid rafts contribute to the detergent resistance of merlin and is consistent with the observation by other investigators that the effect of CD is not quantitative (36). Although the change in detergent solubility of merlin after disruption of lipid rafts was modest, the buoyancy of merlin, as seen by Optiprep gradient centrifugation, was altered significantly. As shown in Fig. 2*C*, CD treatment eliminated the presence of merlin in the 20% fraction, greatly reduced its flotation into the 25% fraction, and enhanced its presence in the 30% fraction, thus confirming that flotation of merlin in density gradients is dependent on intact DRMs. Importantly, only a very small amount of merlin shifted to the TX-100-soluble 35% fraction, and no merlin shifted into the 40% fraction on CD treatment, consistent with the observation that CD exposure does not render merlin quantitatively detergent soluble.

Lipid rafts and caveolae are the two major classes of DRMs. To explore whether merlin was localized to lipid rafts, caveolae, or both, U251 cells expressing merlin-eGFP were extracted with TX-100 and examined by confocal microscopy after staining for a lipid raft marker, Fyn, or a marker for caveolae, caveolin. Merlin colocalized with the lipid raft marker Fyn (Fig. 3*A*), with some cells showing virtually complete coincidence of fluorescence. Images at higher magnification (Fig. 3*B*) demonstrate colocalization at the level of individual puncta. In contrast, overlap of merlin with caveolin was minimal and confined to the edges of the cell (Fig. 3*C*, *left panel*). Elsewhere in the cell, merlin- and caveolin-containing puncta did not coincide, as is evident in high-magnification images (Fig. 3*C*, *right panel*). Thus, the bulk of the punctate, TX-100-insoluble merlin, was localized to lipid rafts, not caveolae.

What might be the physiological significance of the residence of merlin in lipid rafts? Lipid rafts are widely recognized to be sites of concentration of signaling molecules and, as such, serve to enhance the efficiency of signal transduction events. Because merlin is known to inhibit signaling pathways leading to cell growth (7), we thus explored the extent to which merlin resided in lipid rafts under proliferative and growth-suppressive conditions.

NIH3T3 fibroblasts, a system used extensively for studying merlin function (11), were used to determine whether residence of merlin in lipid rafts was sensitive to its functional state. One million NIH3T3 fibroblasts were plated onto 100- and 35-mm tissue culture dishes and allowed to adhere overnight. Cells were then transfected with merlin-eGFP and returned to the incubator for an additional 24 h. At the end of this period, the cells in the 35-mm dish were fully confluent, with all cells being in contact with their neighbors (a condition shown to favor the active form of merlin), whereas very little cell-cell contact was seen among the cells in the 100-mm dish (a condition shown to favor the inactive form of merlin).

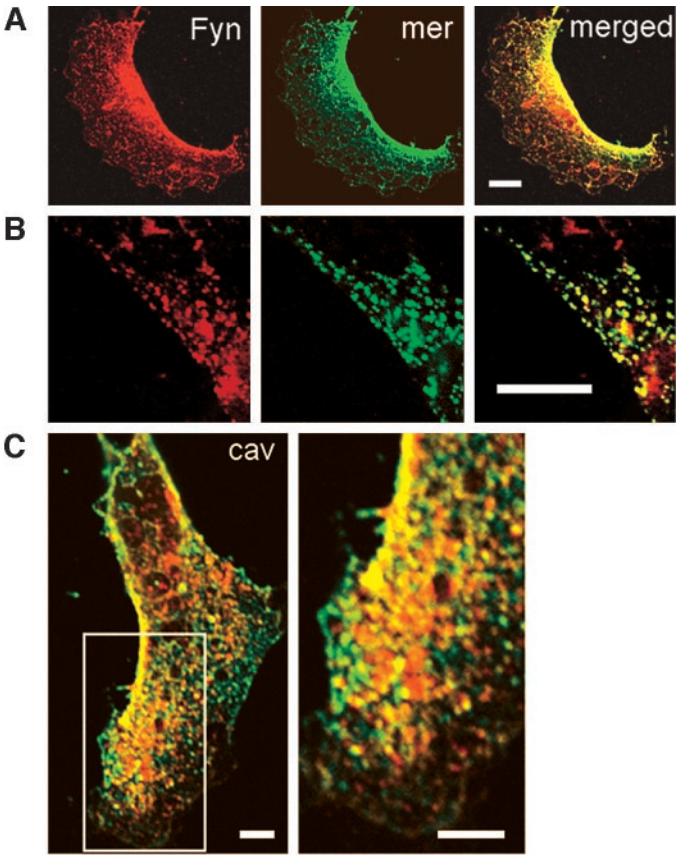

Fig. 3. Merlin colocalizes with lipid rafts but not caveolae. U251 cells expressing merlin-enhanced green fluorescent protein were labeled with an anti-Fyn (*A* and *B*) or anti-caveolin (*C*) antibody after detergent extraction and fixation and then examined by confocal microscopy. Control staining that lacked primary antibody but included secondary antibody showed no fluorescence (data not shown). Fyn and caveolin are in *red*, merlin is in *green*, and areas of colocalization appear *yellow*. The boxed area in the *left panel* of *C* is enlarged in the *right panel*. The *scale bar* represents 10 μm for *A* and the *left panel* of *C* and 5 μm for *B* and the *right panel* of *C*.

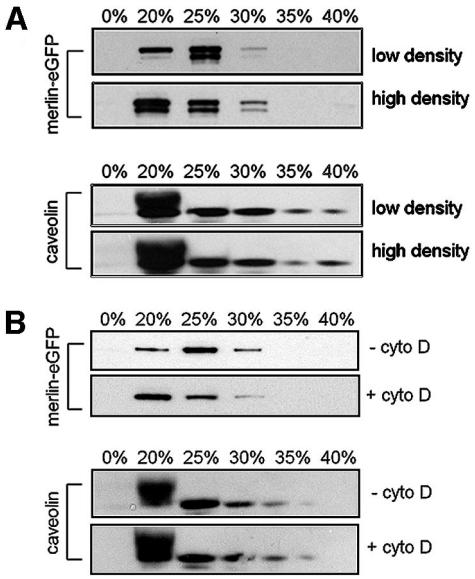

Fig. 4. Increased cell density or disruption of microfilaments increases the buoyancy of merlin. In *A* and *B*, the *top pair* of blots was probed for merlin, and the *bottom pair* was probed for caveolin as a control for a detergent-resistant membrane-associated protein. *A*, 10^6 NIH3T3 cells were plated on 100- or 35-mm plates as described in "Materials and Methods" to create low and high cell density growth conditions, respectively. After 24 h, cells were transiently transfected with merlin-enhanced green fluorescent protein and returned to the incubator for an additional 24 h before Optiprep fractionation. Note the shift of merlin into the 20% fraction when cells were grown to high density, whereas the flotation of caveolin was unaffected by changes in cell density. *B*, to disrupt F-actin, U251 cells were treated with 10 μM cytochalasin D 90 min before gradient centrifugation (+*cyto D*). Vehicle-treated control cells are labeled −*cyto D*. Note the increased amount of merlin in the 20% fraction in treated cells. In contrast, the flotation of caveolin is unaffected by F-actin disruption.

By density gradient centrifugation analysis, all of the merlin was resistant to TX-100 solubilization under both growth conditions, as evidenced by its continued presence in DRM fractions. However, under low cell density conditions, which favored inactivation of merlin, the bulk of the merlin appeared in the 25% Optiprep fraction, with a trace amount in the 20% Optiprep fraction (Fig. 4*A*). In contrast, merlin from cells grown to confluence (which favored activation of merlin) showed an increased presence in the 20% Optiprep fraction, with trailing amounts in the 25% fraction and a minute amount in the 30% fraction. Thus, whereas the solubility of merlin did not change with cell density, and the preponderance of merlin resided in lipid rafts regardless of cell density, activated, growth-suppressive merlin has higher buoyancy than functionally inactive, growth-permissive merlin. One possible explanation for this behavior is that with the transition to a growth-suppressive state, merlin dissociates from one or more binding partners that affect its buoyancy without affecting its attachment to lipid rafts. This interpretation is consistent with a recent report by Nebl *et al.* (35), in which the authors describe a less buoyant subset of DRMs in bovine neutrophils (DRM-H) that contain bound cytoskeletal proteins such as β-fodrin and actin.

Because merlin is believed to dissociate from actin-based structures when it assumes its active, growth-suppressive (*i.e.*, closed) conformation (11), we hypothesized that the less buoyant merlin seen at low cell density could be due to direct or indirect association with the F-actin cytoskeleton when merlin is in the open conformation. To test directly whether the flotation of merlin is influenced by the actin cytoskeleton, we treated subconfluent merlin-eGFP-expressing U251 cells with cytochalasin D to disrupt their microfilament network and then suspended the cells in cold 1% TX-100 and subjected them to gradient centrifugation analysis. As shown in Fig. 4*B*, F-actin disruption before gradient fractionation increased the abundance of merlin in the 20% fraction and correspondingly decreased the abundance in the 25% and 30% fractions. This increase in merlin buoyancy is nearly identical to what was observed in cells favoring active merlin (Fig. 4*A*). Because merlin appears to be localized to lipid rafts regardless of whether the actin cytoskeleton is intact or not, it is likely that the increase in merlin buoyancy that occurs after cytochalasin treatment reflects the dissolution of a physical link between the actin cytoskeleton and merlin-containing lipid rafts. Accordingly, the increase in merlin buoyancy in cells grown to high density is likely the result of merlin adopting the closed conformation and its concomitant dissociation from the microfilament network.

To further test whether the interconversion of merlin between the active and inactive conformation induced changes in its lipid raft interactions, we used an established experimental paradigm to model the opening and closing of ERM proteins and merlin (10, 37). In this system, expressing each half-molecule separately mimics the inactive, open conformation, whereas coexpression of the two halves allows their interaction, reconstituting the closed conformation. Sherman *et al.* (10) demonstrated that coexpression of the NH_2- and COOH-terminal halves of merlin results in a functionally active, growth-suppressive molecule, whereas each half expressed separately has no effect on cell growth.

We created T7 and hemagglutinin epitope-tagged expression constructs for the NH_2- and COOH-terminal halves of merlin, respectively, and expressed them either individually or together in NIH3T3 cells. When expressed individually in NIH3T3 cells, both the NH_2- and COOH-terminal halves of merlin localized to the detergent-resistant fraction of P100 (Fig. 5*A*, *top panel*), with trace amounts of the NH_2-terminal half appearing in the cytosolic and TX-100-soluble fractions. This result is consistent with the presence of membrane-associating domains in both the NH_2- and COOH-terminal halves. Optiprep gradient analysis showed that both halves were predominantly in the 25% DRM fraction (Fig. 5*B*, *top panel*). These results suggest that each half of the merlin molecule, in addition to simple membrane targeting elements, also possesses lipid raft targeting information and support our hypothesis that the open, inactive conformation of merlin resides in "heavy" lipid rafts.

When coexpressed, the two halves of merlin cofractionated in both the detergent solubilization (Fig. 5*A*) and Optiprep (Fig. 5*B*) assays, suggesting they are bound to one another, forming the closed conformation as reported previously (10). The coexpressed half-molecules remained in the P100 fraction, with a significant increase in the amount of protein soluble in TX-100 and n-OG (Fig. 5*A*, *bottom panel*), supporting the notion that closing of merlin does not cause it to be released into the cytosol. In Optiprep gradients (Fig. 5*B*, *bottom panel*), both halves of merlin migrated from the detergent-resistant heavy rafts (25% Optiprep) into lighter rafts (20% Optiprep) and TX-100-soluble portions of the plasma membrane (30–40% Optiprep). In summary, our results support a model whereby activation of merlin results in a shift of merlin from heavy rafts to lighter rafts (Fig. 6).

DISCUSSION

The Physiological Significance of Merlin Lipid Raft Localization. We have presented evidence that the tumor suppressor protein merlin is constitutively localized to lipid rafts. The evidence is 3-fold: merlin colocalizes with a lipid raft marker, Fyn; has limited solubility in cold TX-100; and has buoyancy in a density gradient expected of a lipid raft resident protein. In contrast, its close relative in the ERM

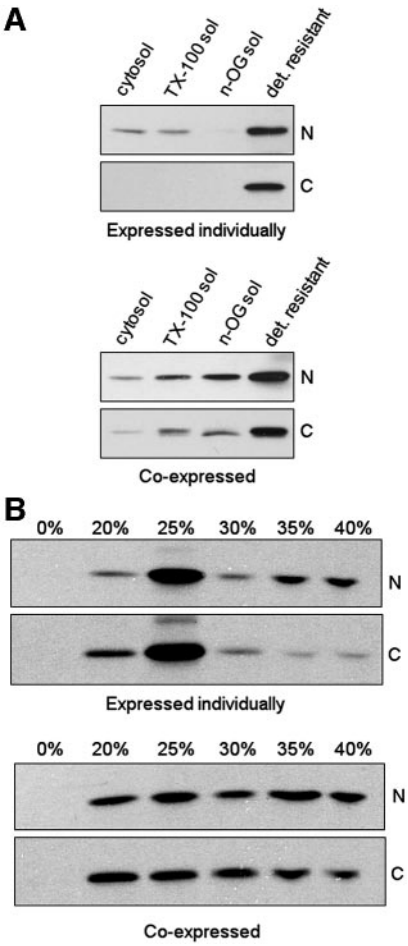

Fig. 5. Merlin translocates between different classes of lipid rafts as cell density changes. NIH3T3 cells (10^6) on 60-mm dishes were transfected with NH_2-or COOH-terminal expression constructs and subjected to sequential detergent fractionation (*A*) or Optiprep gradient fractionation (*B*). When expressed individually, the two halves of merlin mimic the behavior of full-length merlin at low cell density (*i.e.*, the open, inactive conformation). However, when coexpressed, the NH_2- and COOH-terminal halves approximate the flotation and solubility behavior of active merlin.

family, ezrin, is almost completely cytosolic (Fig. 2) and behaves as a cytosolic protein in density gradient centrifugation.

There is suggestive evidence from previous genetic studies that the localization of merlin to lipid rafts may be of physiological significance. Patient mutations in *NF2* have been identified that encode merlin proteins with increased solubility in TX-100 (15, 21). Although this has been attributed to dissociation from the cytoskeleton (15, 21), it is equally tenable that it stems from attenuation of merlin-lipid raft association. Indeed, we have shown that intact microfilaments are not required for the TX-100 detergent resistance of merlin (Fig. 4*B*). We are currently working to determine whether TX-100-soluble mutant merlin proteins show decreased affinity for lipid rafts.

The observation that merlin is constitutively resident in regions of the plasma membrane known to harbor a plethora of signaling molecules (31) is entirely consistent with its known function as a tumor suppressor. In fact, the small GTPase Rac, to which merlin has been functionally linked (11, 14), has been identified as a lipid raft component as well (38, 39). Therefore, the key components of at least one merlin-mediated signaling pathway are lipid raft resident. It remains to be determined whether other upstream and downstream members of this pathway also reside in lipid rafts.

Although merlin is constitutively localized to lipid rafts, gradient centrifugation analysis revealed that this localization is quite dynamic and likely related to the function of merlin as a regulator of cell growth. When cells grew to high density, merlin shifted from a heavier to a lighter lipid raft-containing fraction (Fig. 4*A*), and a similar shift occurred when the NH_2-terminal and COOH-terminal halves of merlin were coexpressed in the same cells (Fig. 5*B*). High cell density favors the active, growth-suppressive, closed conformation of merlin (12, 40), and coexpression of the NH_2-terminal and COOH-terminal half-molecules is an experimental paradigm that has been shown to mimic the closed (active) state of merlin (10). When cells were treated with cytochalasin D before gradient fractionation, a similar shift of merlin to a lighter raft fraction was also seen (Fig. 4*B*), suggesting that partial disassembly of the F-actin cytoskeleton leads to physical detachment of merlin from the cytoskeleton. Taken together, our data support a model whereby, in its transition from being growth permissive to growth suppressive, merlin dissociates from a less buoyant, actin-rich, lipid raft complex and enters another subset of rafts that are more buoyant (Fig. 6). Indeed, the translocation of proteins between different subsets of lipid rafts is thought to be one mechanism by which signaling pathways are regulated because the translocation may allow a given protein to initiate or terminate an interaction with another protein (41).

Interestingly, the coexpression of merlin half-molecules was dissimilar to the expression of the full-length merlin molecule in one respect. When coexpressed in cells, the two halves of merlin exhibited greater TX-100 solubility than when they were expressed individually (Fig. 5). In contrast, full-length merlin does not become more soluble under any condition. This may be because protein conformation and dynamics of the full-length molecule are not fully approximated by the two half-molecules bound to one another. Additionally, the full-length molecule may possess capacity for interaction with raft proteins that is lost with coexpression of half-molecules. Alternatively, it is possible that the coexpressed half-molecules associate and dissociate in a steady state; once dissociated, the probability of re-binding may be less than that of the re-closing of the full-length molecule after opening.

Other facets of merlin function may also be dependent on its localization to lipid rafts. Merlin has been localized to endosomes (42), and recent work has shown that many clathrin-independent endocytic processes occur from lipid rafts (43). In $Nf2^{-/-}$ mouse embryo fibroblasts, adherens junctions are destabilized as a result of loss of merlin (44). Interestingly, many members of the cadherins superfamily of junctional proteins interact with the Src family kinase, Fyn, and are localized to lipid rafts (45). Additionally, merlin has been

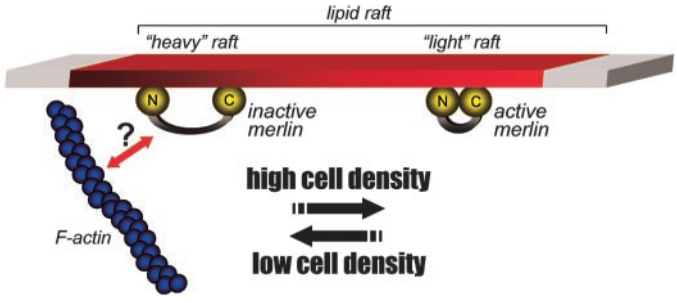

Fig. 6. Model for merlin activation in lipid rafts. In our model, merlin is constitutively localized to lipid rafts. At low cell density, when the inactive form of merlin is favored, merlin is likely to be in an open conformation. In this state, merlin is associated either directly or indirectly (unknown mechanism denoted by *question mark*) with the F-actin cytoskeleton. At high cell density, merlin switches to the active (closed) conformation, which is promoted by intramolecular association. During this transition, merlin loses association with the F-actin network but continues to remain in lipid rafts.

shown to participate in signal transducers and activators of transcription (STAT) signaling (46). STAT proteins also are raft resident (47), so it is conceivable that raft localization of merlin is important for this function as well.

How Is Merlin Targeted to Rafts? A question of considerable interest is how merlin is targeted to lipid rafts. Transfection studies of constructs encoding the NH_2-terminal and COOH-terminal halves of merlin indicate that both halves reside in lipid rafts when expressed individually, suggesting that both halves contain raft-targeting sequences (Fig. 5). The biochemical basis for raft targeting could be protein-protein or protein-lipid interactions (31). In the case of merlin, the FERM domain, putative actin-binding sites, and the binding sites for phosphatidylinositol 4,5-bisphosphate in the NH_2-terminal half, as well as the βII-spectrin-binding site in the COOH-terminal half, all represent potential candidates for binding proteins or lipids that may anchor merlin to lipid rafts. Current studies in our laboratory are directed at defining the precise sequence requirements for raft targeting.

In our initial screen of proteins that might anchor merlin to lipid rafts, we found that three putative merlin-binding proteins, CD44 (12, 48), β_1 integrin (49, 50), and paxillin (51), were not required for merlin to be in lipid rafts. In fact, these three proteins were found to be Triton soluble in Optiprep gradients under the same conditions in which merlin was raft associated (data not shown). These observations are consistent with a recent report by Lallemand *et al.* (44), who showed that loss of contact-dependent growth arrest in $Nf2^{-/-}$ mouse embryo fibroblasts was independent of CD44 and also failed to detect interaction between merlin and paxillin in the same cells. Thus, cellular factors responsible for merlin raft localization have yet to be identified.

To our knowledge, merlin is the first tumor suppressor localized to lipid rafts. Lipid rafts have been widely considered as regions that positively influence cell growth (31), and the presence of merlin within them demonstrates that growth-inhibitory signals can also be found within these specialized membrane microdomains. The constitutive localization of merlin to rafts is likely to be crucial for the ability of merlin to intercede and disrupt positive growth cues emanating from the plasma membrane.

ACKNOWLEDGMENTS

We thank Dr. Nancy Kleene (Center for Biological Microscopy, University of Cincinnati) for expert assistance with confocal microscopy and Drs. Robert Brackenbury, Karen Knudsen, and Pierig Lepont for critical reading of the manuscript.

REFERENCES

1. Rouleau GA, Merel P, Lutchman M, et al. Alteration in a new gene encoding a putative membrane-organizing protein causes neuro-fibromatosis type 2. Nature (Lond) 1993;363:515–21.
2. Trofatter JA, MacCollin MM, Rutter JL, et al. A novel moesin-, ezrin-, radixin-like gene is a candidate for the neurofibromatosis 2 tumor suppressor. Cell 1993;72:791–800.
3. McClatchey AI, Saotome I, Ramesh V, Gusella JF, Jacks T. The Nf2 tumor suppressor gene product is essential for extraembryonic development immediately prior to gastrulation. Genes Dev 1997;11:1253–65.
4. McClatchey AI, Saotome I, Mercer K, et al. Mice heterozygous for a mutation at the Nf2 tumor suppressor locus develop a range of highly metastatic tumors. Genes Dev 1998;12:1121–33.
5. Giovannini M, Robanus-Maandag E, van der Valk M, et al. Conditional biallelic Nf2 mutation in the mouse promotes manifestations of human neurofibromatosis type 2. Genes Dev 2000;14:1617–30.
6. den Bakker MA, Vissers KJ, Molijn AC, et al. Expression of the neurofibromatosis type 2 gene in human tissues. J Histochem Cytochem 1999;47:1471–80.
7. Bretscher A, Chambers D, Nguyen R, Reczek D. ERM-Merlin and EPB50 protein families in plasma membrane organization and function. Annu Rev Cell Dev Biol 2000;16:113–43.
8. Meng J-J, Lowrie DJ, Sun H, et al. Interaction between two isoforms of the NF2 tumor suppressor protein, Merlin, and between Merlin and Ezrin, suggests modulation of ERM proteins by Merlin. J Neurosci Res 2000;62:491–502.
9. Gronholm M, Sainio M, Zhao F, et al. Homotypic and heterotypic interaction of the neurofibromatosis 2 tumor suppressor protein merlin and the ERM protein ezrin. J Cell Sci 1999;112:895–904.
10. Sherman L, Xu, H-M, Geist RT, et al. Interdomain binding mediates tumor growth suppression by the NF2 gene product. Oncogne 1997;15:2505–9.
11. Shaw RJ, Paez JG, Curto M, et al. The Nf2 tumor suppressor, merlin, functions in Rac-dependent signaling. Dev Cell 2001;1:63–72.
12. Morrison H, Sherman LS, Legg J, et al. The NF2 tumor suppressor gene product, merlin, mediates contact inhibition of growth through interactions with CD44. Genes Dev 2001;15:968–80.
13. Gonzalez-Agosti C, Xu L, Pinney D, et al. The merlin tumor suppressor localizes preferentially in membrane ruffles. Oncogene 1996;13:1239–47.
14. Pelton PD, Sherman LS, Rizvi TA, et al. Ruffling membrane, stress fiber, cell spreading, and proliferation abnormalities in human Schwannoma cells. Oncogene 1998;17:2195–209.
15. Stokowski RP, Cox DR. Functional analysis of the neurofibromatosis type 2 protein by means of disease-causing point mutations. Am J Hum Genet 2000;66:873–91.
16. Schulze KMM, Hanemann CO, Muller HW, Hanenberg H. Transduction of wild-type merlin into human Schwannoma cells decreases Schwannoma cell growth and induces apoptosis. Hum Mol Genet 2002;11:69–76.
17. Bashour A-M, Meng J-J, Ip W, MacCollin M, Ratner N. The neurofibromatosis type 2 gene product, merlin, reverses the F-actin cytoskeletal defects in primary human Schwannoma cells. Mol Cell Biol 2002;22:1150–7.
18. Bretscher A, Edwards K, Fehon RG. ERM proteins and merlin: integrators at the cell cortex. Nat Rev Mol Cell Biol 2002;3:586–99.
19. James MF, Manchanda N, Gonzalez-Agosti C, Hartwig JH, Ramesh V. The neurofibromatosis 2 protein product merlin selectively binds F-actin but not G-actin, and stabilizes the filaments through a lateral association. Biochem J 2001;356:377–86.
20. den Bakker MA, Riegman PH, Suurmeijer AP, et al. Evidence for a cytoskeleton attachment domain at the N-terminus of the NF2 protein. J Neurosci Res 2000;62:764–71.
21. Deguen B, Merel P, Goutebroze L, et al. Impaired interaction of naturally occurring mutant NF2 protein with actin-based cytoskeleton and membrane. Hum Mol Genet 1998;7:217–26.
22. Simons K, Ikonen E. Functional rafts in cell membranes. Nature (Lond) 1997;387:569–72.
23. den Bakker MA, Tascilar M, Riegman PH, et al. Neurofibromatosis type 2 protein co-localizes with elements of the cytoskeleton. Am J Pathol 1995;147:1339–49.
24. Oliferenko S, Paiha K, Harder T, et al. Analysis of CD44-containing lipid rafts: recruitment of Annexin II and stabilization by the actin cytoskeleton. J Cell Biol 1999;146:843–54.
25. Stickney JT, Buss JE. Murine guanylate-binding protein: incomplete geranylgeranyl isoprenoid modification of an interferon-γ-inducible guanosine triphosphate-binding protein. Mol Biol Cell 2000;11:2191–200.
26. Schmucker B, Ballhausen WG, Kressel M. Subcellular localization and expression pattern of the neurofibromatosis type 2 protein merlin/schwannomin. Eur J Cell Biol 1997;72:46–53.
27. Sainio M, Zhao F, Heiska L, et al. Neurofibromatosis 2 tumor suppressor protein colocalizes with ezrin and CD44 and associates with actin-containing cytoskeleton. J Cell Sci 1997;110:2249–60.
28. Xu H-M, Gutmann DH. Merlin differentially associates with the microtubule and actin cytoskeleton. J Neurosci Res 1998;51:403–15.
29. Yuan H, Takeuchi E, Salant DJ. Podocyte slit-diaphragm protein nephrin is linked to the actin cytoskeleton. Am J Physiol Renal Physiol 2002;282:F585–91.
30. Brown DA, London E. Functions of lipid rafts in biological membranes. Annu Rev Cell Dev Biol 1998;14:111–36.
31. Simons K, Toomre D. Lipid rafts and signal transduction. Nat Rev Mol Cell Biol 2000;1:31–9.
32. Brown DA, Rose JK. Sorting of GPI-anchored proteins to glycolipid-enriched membrane subdomains during transport to the apical cell surface. Cell 1992;68:533–44.
33. Bretscher A, Gary R, Berryman M. Soluble ezrin purified from placenta exists as stable monomers and elongated dimers with masked C-terminal ezrin-radixin-moesin association domains. Biochemistry 1995;34:16830–7.
34. Tomas EM, Chau TA, Madrenas J. Clustering of a lipid-raft associated pool of ERM proteins at the immunological synapse upon T cell receptor or CD28 ligation. Immunol Lett 2002;83:143–7.
35. Nebl T, Pestonjamasp KN, Leszyk JD, et al. Proteomic analysis of a detergent-resistant membrane skeleton from neutrophil plasma membranes. J Biol Chem 2002;277:43399–409.
36. Ilangumaran S, Hoessli D. Effects of cholesterol depletion by cyclodextrin on the sphingolipid microdomains of the plasma membrane. Biochem J 1998;335:433–40.
37. Gary R, Bretscher A. Ezrin self-association involves binding of an N-terminal domain to a normally masked C-terminal domain that includes the F-actin binding site. Mol Biol Cell 1995;6:1061–75.
38. Kumanogoh H, Miyata S, Sokawa Y, Maekawa S. Biochemical and morphological analysis on the localization of Rac1 in neurons. Neurosci Res 2001;39:189–96.

39. Li N, Mak A, Richards DP, et al. Monocyte lipid rafts contain proteins implicated in vesicular trafficking and phagosome formation. Proteomics 2003;3:536–48.
40. Shaw RJ, McClatchey AI, Jacks T. Regulation of the neurofibromatosis type 2 tumor suppressor protein, Merlin, by adhesion and growth arrest stimuli. J Biol Chem 1998;273:7757–64.
41. Simons K, Ehehalt R. Cholesterol, lipid rafts, and disease. J Clin Investig 2002;110: 597–603.
42. McCartney BM, Fehon RG. Distinct cellular and subcellular patterns of expression imply distinct functions for the Drosophila homologues of moesin and the neufibromatosis 2 tumor suppressor, Merlin. J Cell Biol 1996;133:843–52.
43. Nabi IR, Le PU. Caveolae/raft-dependent endocytosis. J Cell Biol 2003;161:673–7.
44. Lallemand D, Curto M, Saotome I, Giovannini M, McClatchey AI. NF2 deficiency promotes tumorigenesis and metastasis by destabilizing adherens junctions. Genes Dev 2003;17:1090–100.
45. Angst BD, Marcozzi C, Magee AI. The cadherin superfamily: diversity in form and function. J Cell Sci 2001;114:629–41.
46. Scoles DR, Nguyen VD, Qin Y, et al. Neurofibromatosis 2 (NF2) tumor suppressor schwannomin and its interacting protein HRS regulate STAT signaling. Hum Mol Genet 2002;11:3179–89.
47. Sehgal PB, Guo GG, Shah M, Kumar V, Patel K. Cytokine signaling: STATS in plasma membrane rafts. J Biol Chem 2002;277:12067–74.
48. Tsukita S, Oishi K, Sato N, et al. ERM family members as molecular linkers between the cell surface glycoprotein CD44 and actin-based cytoskeletons. J Cell Biol 1994; 126:391–401.
49. Obremski VJ, Hall AM, Fernandez-Valle C. Merlin, the neurofibromatosis type 2 gene product, and β_1 integrin associate in isolated and differentiating Schwann cells. J Neurobiol 1996;37:487–501.
50. Denisenko-Nehrbass N, Goutebroze L, Galvez T, et al. Association of Caspr/paranodin with tumour suppressor schwannomin/merlin and β_1 integrin in the central nervous system. J Neurochem 2003;84:209–21.
51. Fernandez-Valle C, Tang Y, Ricard J, et al. Paxillin binds schwannomin and regulates its density-dependent localization and effect on cell morphology. Nat Genet 2002;31:354–62.